Advances in Forest Fire Research 2018

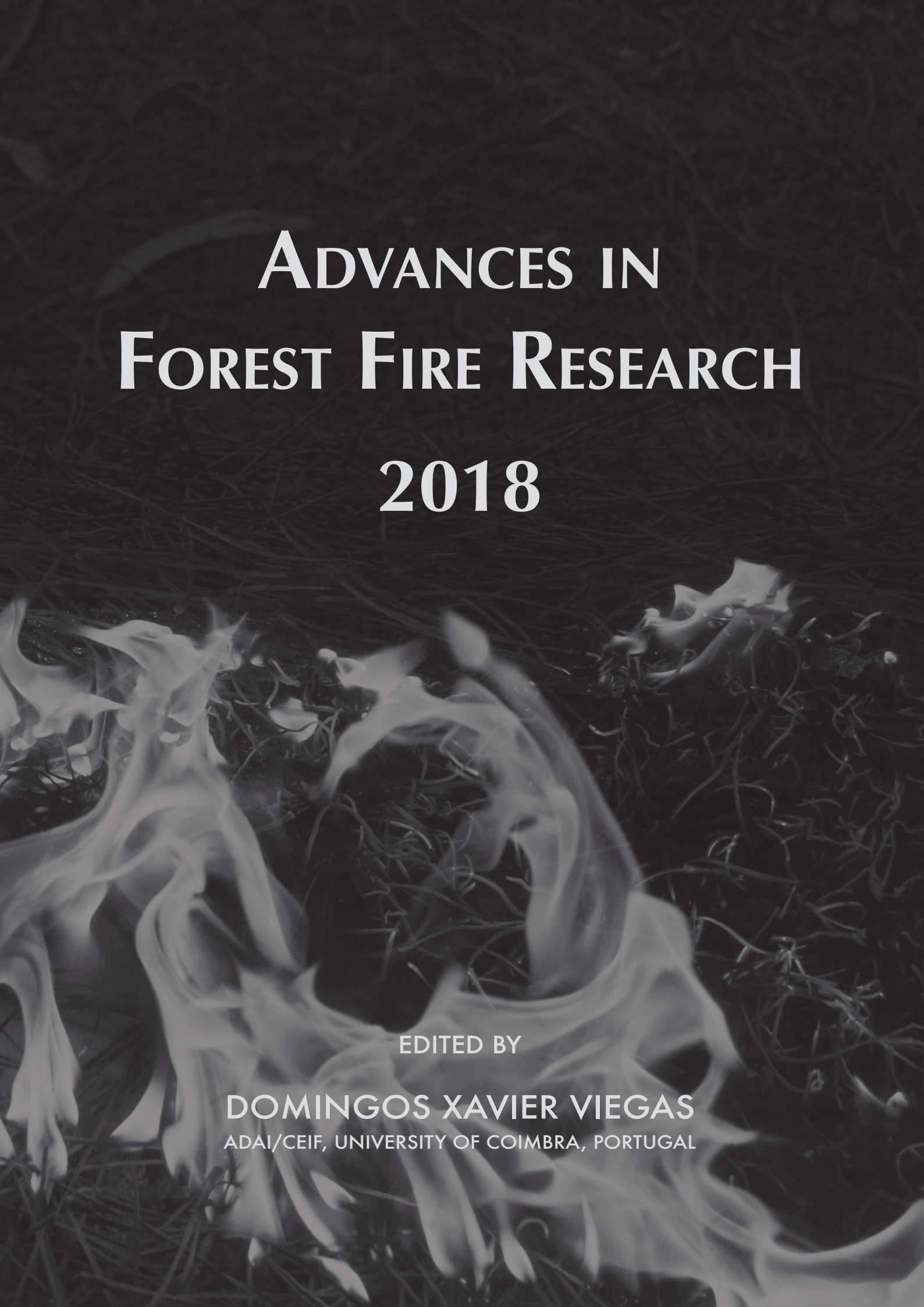

EDITED BY

DOMINGOS XAVIER VIEGAS

ADAI/CEIF, UNIVERSITY OF COIMBRA, PORTUGAL

Advances in Forest Fire Research 2018 - D. X. Viegas (Ed.)
Chapter 3 – Fire Management
https://doi.org/10.14195/978-989-26-16-506_64

New Lagrangian surface forest fire propagation model

M. Ambroz*, K. Mikula

Department of Mathematics and Descriptive Geometry, Faculty of Civil Engineering, Slovak University of Technology, Radlinského 11, 810 05 Bratislava, Slovak Republic, {ambroz.martin.ml@gmail.com, mikula@math.sk}*

Abstract

We introduce new Lagrangian surface forest fire spread model, which is based on the evolution of a three dimensional surface curve representing the fire perimeter on the topography. We split the general motion of any point of the surface curve into the normal and tangential directions. The velocity in the normal direction is given by the rate of spread, i.e. it depends on the local characteristics of fuel, terrain slope, wind speed and velocity and shape of the fire perimeter with respect to the topography (geodesic and normal curvature). The velocity in the tangential direction, which does not change the shape of the fire perimeter, is used to redistribute the curve points asymptotically uniform along the curve. This surface curve is projected into the horizontal plane as a planar curve, which evolution is numerically computed and evolved curve is mapped back to the surface. For the numerical computations we discretize the arising intrinsic partial differential equation by a semi-implicit scheme in curvature term and for the advection term we use the so-called inflow-implicit/outflow-explicit approach and implicit upwind technique which guarantee solvability of linear systems by efficient tridiagonal solver without any time step restriction and robustness with respect to singularities. Our fast and reliable treatment of topological changes (splitting and merging of the curves) with computational complexity *O(n)* is described and presented on examples as well. We demonstrate the influence of the fire spread model parameters on a testing and real topography.

Keywords: forest fire modelling, surface curve, curve evolution, topological changes, inverse modelling

1. Introduction

In the mathematical literature, there exists a number of studies about the evolution of planar and surface curves with many various applications. We distinguish two main approaches to handle the curve evolution problems, the so-called Lagrangian (direct or vector-based) approach, see e.g. (Dziuk, 1999), (Mikula & Ševčovič, 2004), (Balažovjech, et al., 2012) and the so-called Eulerian (level-set or raster-based) approach, see e.g. (Sethian, 1999), (Osher & Fedkiw, 2002). In the Eulerian level-set approach, one solves the problem of curve evolution in a 2-D computational domain which is usually discretized by a uniform grid and the number of discrete unknowns is proportional to the number of such 2-D grid points. The evolving curve is then obtained implicitly, as the zero isoline of 2-D + time level set function. In the Lagrangian approach one evolves directly the curve discretization points, so it is spatially 1-D problem and thus computationally much simpler and faster than the level-set method. However, the Lagrangian approaches need the so-called tangential grid point redistribution (Hou, et al., 1994), (Barrett, et al., 2009), (Mikula & Ševčovič, 2001), (Mikula & Urbán, 2012) and efficient algorithm for the detection and treatment of topological changes during the evolution (Balažovjech, et al., 2012), (Mikula & Urbán, 2012), (Benninghoff & Garcke, 2014), which are on the other hand automatically handled by the level set method (Sethian, 1999), (Osher & Fedkiw, 2002). When the Lagrangian methods are tangentially stabilized and are able to treat the topological changes fastly, they represent really efficient approaches to 2-D or surface curve evolution

We introduce a new surface forest fire spread model, which is based on the evolution of a three dimensional surface curve representing the fire perimeter on the topography. The mathematical model for curve evolution is based on the empirical laws of the fire propagation influenced by fuel, wind,

terrain slope and the fire perimeter shape with respect to the topography (geodesic and normal curvature). Our fast treatment of topological changes (splitting and merging of the curves) is described and presented on examples as well. We demonstrate the influence of the fire spread model parameters on a testing and real topography and we reconstruct a simulated grassland fire.

2. Surface forest fire propagation model

In our model we use the so-called Lagrangian approach to the evolution of a surface curve, representing a fire perimeter. The surface is given as a graph of a discrete topography function $\varphi(\mathbf{x}) = \varphi(x,y)$, which is given, e.g., by a digital model of terrain. The discrete surface curve points $\mathbf{X} = (\mathbf{x}, \varphi(\mathbf{x}))$ are evolving in the normal direction, given by outer unit normal vector $\mathcal{N}$ by following formula

$$\mathbf{X}_t = \mathcal{V}\mathcal{N}\,, \tag{1}$$

where $\mathcal{V}$ is the normal velocity of the 3-D surface curve. The outer unit normal vector $\mathcal{N}$ is given as $\mathcal{N} = \mathcal{T} \times \mathcal{N}_\mathcal{M}$, where $\mathcal{T} = \partial\mathbf{X}/\partial s$, with s being the arc-length parameter and $\mathcal{N}_\mathcal{M} = (1, 0, \partial\varphi/\partial x) \times (0, 1, \partial\varphi/\partial y)$. For better clarity see Figure 1, where we illustrate also the curvature vector $\mathcal{K} = \partial^2\mathbf{X}/\partial s^2$ and its components, geodesic $K_g = \mathcal{K}\cdot\mathcal{N}$ and normal curvature $K_n = \mathcal{K}\cdot\mathcal{N}_\mathcal{M}$, which are useful in the radiation heat influence modeling.

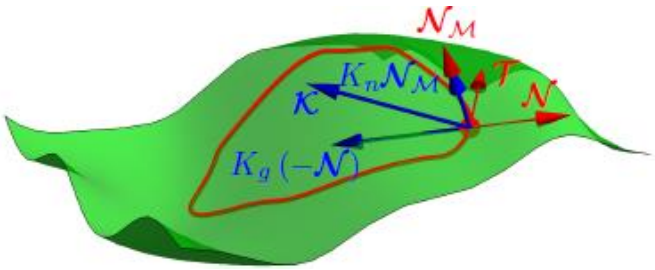

Figure 1 - Surface curve and the outer unit normal vector $\mathcal{N}$, unit tangent vector $\mathcal{T}$, normal to the surface $\mathcal{N}_\mathcal{M}$, curvature $\mathcal{K}$, geodesic curvature K_g and normal curvature K_n.

Design of the normal velocity $\mathcal{V}$ is crucial for a reliable propagation model. We propose a simple formula considering fuel burnability, topography slope, wind velocity and direction and the shape of the fire perimeter with respect to the topography

$$\mathcal{V} = \mathcal{F}\,(\delta_\mathcal{F} - \delta_g K_g + \delta_n K_n)\,, \tag{2}$$

where $\mathcal{F}$ is an external driving force, K_g is a geodesic curvature, K_n is a normal curvature and $\delta_\mathcal{F}$, δ_g and δ_n are weights of the external force, geodesic curvature and normal curvature. This formula provides the dominant role for the external force $\mathcal{F}$ influenced by local fire perimeter shape (K_g and K_n). It also ensures that the fire perimeter will not burn into the unburnable regions due to the curvatures.

Fire perimeters curvature influences the overall rate of spread, see (Weber, 1989) and (Hilton, et al., 2017). In our approach we split the curvature $\mathcal{K}$into geodesic K_g and normal curvature K_n. In case of flat terrain ($K_n = 0$) and linear fire perimeter ($K_g = 0$) the fire spread depends only on the external force $\mathcal{F}$. Considering non-linear fire perimeter, i.e. the curve with convex and concave parts in the tangent plane, the geodesic curvature $K_g \neq 0$. In parts with $K_g < 0$ the fire perimeter is accelerated due to radiant heat accumulation and in parts with $K_g > 0$ the radiation heat dissipation slows down the fire perimeter propagation. If the topography is a valley or a ridge, then $K_n \neq 0$ and it expresses the topography influence to radiation heat transfer. In the valley $K_n > 0$ and causes the fire spread acceleration due to the accumulated radiation heat. On the other hand, on the ridge $K_n < 0$ slows the fire spread down, since the radiation is dissipated.

The external driving force $\mathcal{F}$ is given by the following formula

$$\mathcal{F} = f\, f_w(\mathbf{w}\cdot\mathcal{N})\, f_s(\mathbf{s}\cdot\mathcal{N}), \tag{3}$$

where f is a fuel influence, $f_w(\mathbf{w}\cdot\mathcal{N})$ is a wind influence and $f_s(\mathbf{s}\cdot\mathcal{N})$ is a slope influence on the rate of spread, with $\mathbf{w}$ being a 3-D wind vector, $\mathbf{s}$ being a 3-D slope vector and $\mathcal{N}$ being an outer unit normal vector of the surface curve.

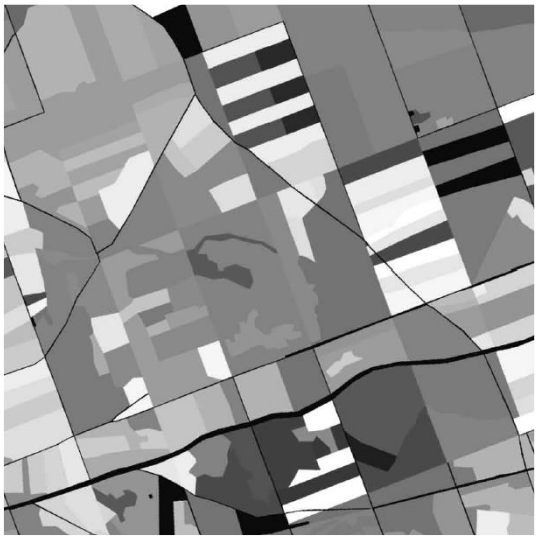

Figure 2 - The example of a 2-D scalar function $f(x)$, created as a weighted combination of selected factors, such as species, age and bulk density.

The fuel influence f is in fact a scalar function $f(\mathbf{x})$ given over the whole computational domain. The values of such scalar function ranges from 0 (black color) to 255 (white color). These values express the spatial variability of rate of spread no wind and flat terrain conditions. According to (Krasnow, et al., 2009) we suppose, that the fuel influence function $f(\mathbf{x})$ is given by a weighted combination of the most important factors, such as species, age, bulk density, fuel moisture, vertical arrangement, fuel loading and compactness. Some of these factors can be determined by a typological forestry maps, like the species, age or bulk density. Their combination creates the fuel influence function $f(\mathbf{x})$, see Figure 2, where the young, dense coniferous forest is considered to be with the highest spread rate.

Wind influence on the fire spread is non-negligible. Wind increases the fuel preheating, drying and it supplies the oxygen to the fire. If the wind direction and fire spread direction are the same, the rate of spread will increase. On the other hand, in case of wind blowing against the fire spread, the rate of spread will decrease. Our model requires the 3-D wind vector $\mathbf{w}$ which we obtain from measured 2-D wind vector $\mathbf{w}^{2D}$ using formula

$$\mathbf{w} = \left(\mathbf{w}^{2D}, \nabla\varphi\cdot\mathbf{w}^{2D}\right)\frac{\left|\mathbf{w}^{2D}\right|}{\sqrt{\left|\mathbf{w}^{2D}\right|^2 + \left(\nabla\varphi\cdot\mathbf{w}^{2D}\right)^2}} \tag{4}$$

Such vector is always parallel to the topography and $|\mathbf{w}| = |\mathbf{w}^{2D}|$. According to (Viegas, et al., 2002), (Scott & Burgan, 2005), the wind influences the rate of spread exponentially, so we consider the scalar product of the wind vector $\mathbf{w}$ and the outer normal vector $\mathcal{N}$ as an exponent of a function $f_w(\mathbf{w}\cdot\mathcal{N})$ in the form

$$f_w\left(\mathbf{w}\cdot\mathcal{N}\right) = e^{\lambda_w(\mathbf{w}\cdot\mathcal{N})}, \tag{5}$$

where λ_w is a positive parameter. If those vectors are perpendicular, $\mathbf{w} \cdot \mathcal{N} = 0$, the external force $\mathcal{F}$ is not influenced by wind, because $f_w = 1$. If the vectors are parallel, $\mathbf{w} \cdot \mathcal{N} = |\mathbf{w}|$, $f_w = e^{\lambda_w |\mathbf{w}|}$, the influence of wind is the strongest. In all other cases, the exponent of the function $f_w(\mathbf{w} \cdot \mathcal{N})$ is given by a projection of the wind vector $\mathbf{w}$ onto the outer normal vector $\mathcal{N}$, see Figure 3.

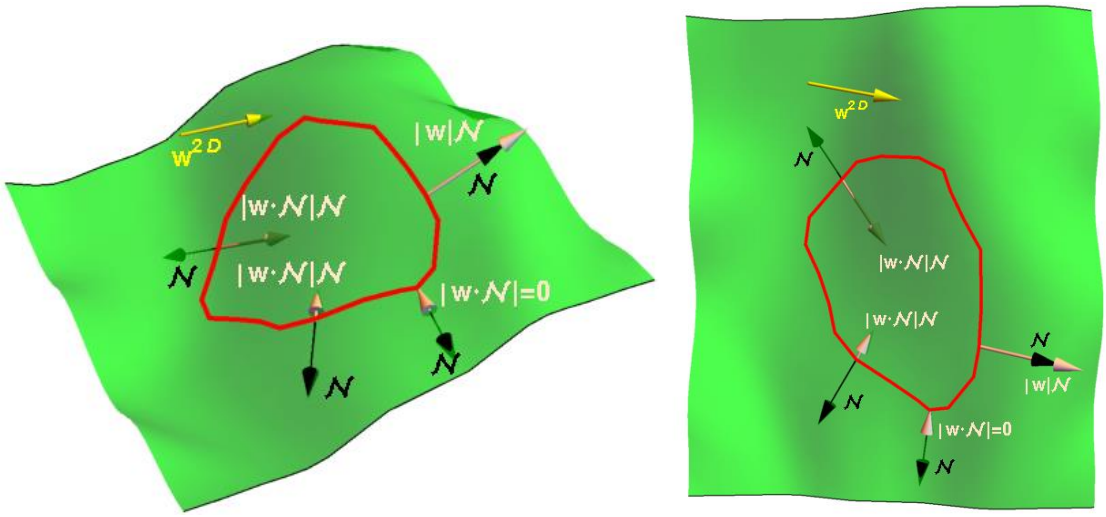

Figure 3 - The example of a projection of the wind vector $\mathbf{w}$ (white) to the normal vector $\mathcal{N}$ (black). The wind vector $\mathbf{w}$ is computed from a measured two-dimensional wind vector $\mathbf{w}^{2D}$ (yellow). Then the dot product $\mathbf{w} \cdot \mathcal{N}$ can result in various cases, including $\mathbf{w} \cdot \mathcal{N} = 0$.

The topography slope increases the radiation and convection heat transfer up the slope. Similarly to wind, slope can increase or decrease the rate of spread. The uphill fire spread rate is increased, while the downhill fire spread is slowed down. The topography slope is given by a gradient of the topography function ∇φ. Since our model requires a 3-D vector of slope, we use formula similar to (4)

$$\mathbf{s} = \left(\nabla\varphi, |\nabla\varphi|^2\right) \frac{|\nabla\varphi|}{\sqrt{|\nabla\varphi|^2 + \left(|\nabla\varphi|^2\right)^2}} = \frac{\left(\nabla\varphi, |\nabla\varphi|^2\right)}{\sqrt{1 + |\nabla\varphi|^2}} . \tag{6}$$

According to (Viegas, et al., 2002), (Scott & Burgan, 2005), (Butler, et al., 2007) the slope influence to the rate of spread is exponential and depends on the projection of the slope vector $\mathbf{s}$ onto the outer normal vector $\mathcal{N}$

$$f_s(\mathbf{s} \cdot \mathcal{N}) = e^{\lambda_s (\mathbf{s} \cdot \mathcal{N})}, \tag{7}$$

where λ_s is a positive parameter.

3. Numerical scheme

For numerical computation we follow (Mikula & Ševčovič, 2006) and we numerically solve the evolution of a projected planar curve. It means, we project the 3-D surface curve into the 2-D planar curve and the evolution is computed for every discrete planar curve point **x** = (x,y). Time evolution of the curve point **x** is given by following formula

$$\mathbf{x}_t = \beta \mathbf{N} + \alpha \mathbf{T}, \tag{8}$$

where β is a planar curve velocity in a direction of is outer unit normal vector **N**, α is a planar curve velocity in a tangent direction, **T** is a unit tangent vector. This formula splits the general motion of any point of the 2-D projected planar curve into the normal and tangential directions. The velocity β in the normal direction **N** changes the shape of the curve. The velocity in the tangential direction, which does not change the shape of the fire perimeter, is used to redistribute the curve points asymptotically uniformly along the curve, where we follow (Mikula & Ševčovič, 2001), (Mikula & Ševčovič, 2004), (Mikula & Ševčovič, 2006), (Mikula & Urbán, 2014).

Our evolution approach allows us to prescribe the normal velocity $\mathcal{V}$ of the 3-D surface curve (in the previous section) and to effectively compute the evolution of the projected 2-D planar curve. To project the normal velocity $\mathcal{V}$ of the surface curve to the normal velocity β of the planar curve we use the formula

$$\beta = \mathcal{V}\sqrt{\frac{1+(\nabla\varphi\cdot\mathbf{T})^2}{1+|\nabla\varphi|^2}}, \tag{9}$$

where ∇φ is a gradient of a topography function φ(**x**).

Numerical discretization is based on the flowing finite volume method. In order to get a discrete form of (8), using the Frenet equation $\mathbf{x}_{ss} = -k\mathbf{N}$ we rewrite (8) to the form of an intrinsic partial differential equation

$$\mathbf{x}_t = \varepsilon\mathbf{x}_{ss} + \alpha\mathbf{x}_s + w\mathbf{x}_s^{\perp}, \tag{10}$$

where

$$\varepsilon = \frac{\mathcal{F}\delta_g}{1+(\nabla\varphi\cdot\mathbf{T})^2}, \tag{11}$$

$$w = \mathcal{F}\left(\delta_{\mathcal{F}}\sqrt{\frac{1+(\nabla\varphi\cdot\mathbf{T})^2}{1+|\nabla\varphi|^2}} + \delta_g\frac{\mathbf{T}^T H(\varphi)\,\mathbf{T}\,(\nabla\varphi\cdot\mathbf{N})}{(1+(\nabla\varphi\cdot\mathbf{T})^2)\,(1+|\nabla\varphi|^2)} + \delta_n\frac{\mathbf{T}^T H(\varphi)\,\mathbf{T}}{\sqrt{1+(\nabla\varphi\cdot\mathbf{T})^2}\,(1+|\nabla\varphi|^2)}\right), \tag{12}$$

$$\alpha_s = \langle k\beta\rangle_\Gamma - k\beta + \omega\left(\frac{L}{g}-1\right), \tag{13}$$

where $\langle k\beta\rangle_\Gamma$ is average value of $k\beta$ along the projected planar curve, k is a curvature of planar curve, ω is parameter determining how fast the redistribution becomes uniform, L is total length of planar curve and g is a so-called local length of 2-D planar cuve, for details see (Ambroz, et al., Submitted).

We use a semi-implicit scheme in curvature term. For the advection term we use the so-called inflow-implicit/outflow-explicit approach (Mikula, et al., 2014) which guarantee solvability of arising linear systems by efficient tridiagonal solver without any computational time step restriction. In the end, we obtain the cyclic tridiagonal system of linear equations

$$A_i^m\mathbf{x}_{i-1}^{m+1} + B\mathbf{x}_i^{m+1} + C_i^m\mathbf{x}_{i+1}^{m+1} = D_i^m \tag{14}$$

$$A_i^m = -\frac{\varepsilon_i^m}{h_i^m} - \frac{b_{i-\frac{1}{2}}^{in}}{2}, \quad C_i^m = -\frac{\varepsilon_i^m}{h_{i+1}^m} - \frac{b_{i+\frac{1}{2}}^{in}}{2}$$

$$B_i^m = \frac{h_{i+1}^m + h_i^m}{2\tau} + \frac{\varepsilon_i^m}{h_i^m} + \frac{\varepsilon_i^m}{h_{i+1}^m} + \frac{b_{i-\frac{1}{2}}^{in}}{2} + \frac{b_{i+\frac{1}{2}}^{in}}{2}$$

$$D_i^m = \mathbf{x}_i^m \frac{h_{i+1}^m + h_i^m}{2\tau} - \frac{b_{i+\frac{1}{2}}^{out}}{2}\left(\mathbf{x}_i^m - \mathbf{x}_{i+1}^m\right) - \frac{b_{i-\frac{1}{2}}^{out}}{2}\left(\mathbf{x}_i^m - \mathbf{x}_{i-1}^m\right) + w_i^m \left(\frac{\mathbf{x}_{i+1}^m - \mathbf{x}_{i-1}^m}{2}\right)^{\perp}.$$

Due to stability reasons, e.g. in case of curve merging, this general numerical scheme is locally replaced by the implicit upwind method.

4. Topological changes

In the Lagrangian approach, there are some issues throughout the curve evolution left to treat additionally. The curve can be self-intersected or can be intersected by another curve. Such self-intersection can occur when the curve velocity is locally slowed down significantly (e.g. nonburnable regions) , see Figure 4. These situations require a topological change, either splitting or merging. However, the detection of such topological changes can be computationally demanding. The most often used strategy of pairwise comparison of grid points have computational complexity $O(n^2)$. In our propagation model we use our $O(n)$ approach, which makes the overall computations fast and reliable in fire perimeter evolution. Our main idea for the topological changes detection, see also (Balažovjech, et al., 2012), is to create an array of cells over the whole computational domain and to check a narrow strip of cells along the curves. In these cells we subsequently check whether there are two non-neighboring points of one curve, which indicates splitting. Similarly we check the cells along the curves, for the case of two points from different curves belonging to one cell. Such situation indicates merging.

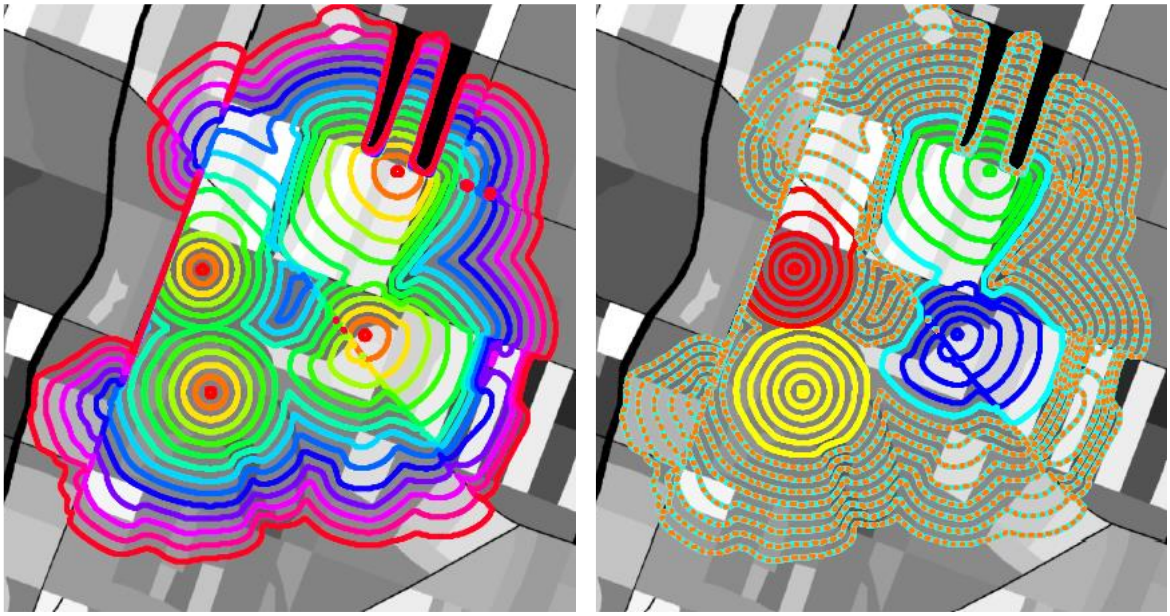

Figure 4 - Merging and splitting of the curves on a ROS map. On the left, four red circles representing the initial fire perimeters and their time evolution is plotted. Curves with the same color represent the fire perimeters position at the same time. On the right, there is the same situation, but the evolution of different fire perimeters is plotted in different color, red, yellow, green and blue, until their merging. After the merging, the color changes to a combination, e.g. green and blue curves merge as a cyan curve.

During the evolution the curve length changes and thus we need to locally add or remove points in order to maintain appropriate number of grid points. Then, the asymptotically uniform redistribution ensures the desired segment length h_d. Thanks to this, we can set the dimensions of the cell along the curves to $2h_d$ x $2h_d$. This ensures maximally 3 neighboring points of smooth curve in one cell.

Basic idea for the splitting detection is to traverse the curve points and mark the cells, where the points belong. First, we mark the cells where all curve points belong by 0. Then we traverse the curve again and we mark the cells by the belonging point number. If a point belongs to a cell already marked by a non-neighboring point the curve will split, since there are more points between the point that entered the cell first time and the point entering the cell again. Those two points in one cell are not necessarily the nearest in their neighboring, thus we find the nearest by pairwise comparing. Then the curve is split in the nearest points into the enlarging (burnt area) and shrinking (unburnt area) curve. The merging detection is very similar. We traverse every curves points and mark the cells, where the points lie by 0. Then we subsequently traverse the curve points again and we mark the cells by the curve number. When a cell is already marked by a different curve the curves will merge, since the points of two curves belong to the same cell. To merge the curve, we find the nearest points between the neighboring points of the points belonging to the same cell.

5. Numerical experiments

In the following experiments we present the behavior of our propagation model on a simple topography. Valley and ridge are given by two planes inclined by 30 degrees from the horizontal plane at both axis direction. The initial fire perimeter is given as a circle in the horizontal plane.

First, we present the influence of the geodesic and normal curvatures on the curve evolution velocity in the valley and on the ridge, see Figure 5. Although those experiments do not simulate the fire behavior (due to a neglected slope influence), they are suitable for the presentation of the heat accumulation or dissipation influencing the rate of spread.

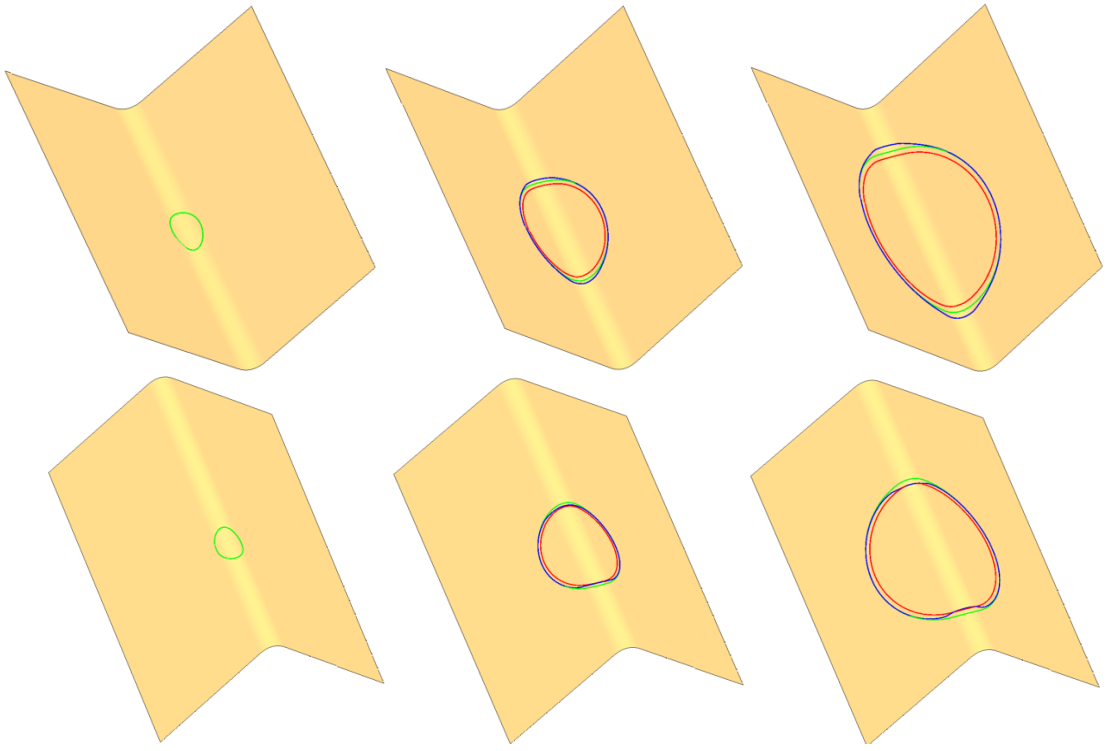

Figure 5 - The comparison of the curve evolution in the valley (top row) and on the ridge (bottom row) driven by unit external force (green) and accompanied by the geodesic curvature (red) or normal curvature (blue). Geodesic curvature slows the curve velocity locally down. The normal curvature speeds the velocity up in the bottom of the valley and slows the velocity down on the top of the ridge.

In the next experiments we simulate the fire spread, considering all the influences in the valley, see Figure 6, and on the ridge, see Figure 7.

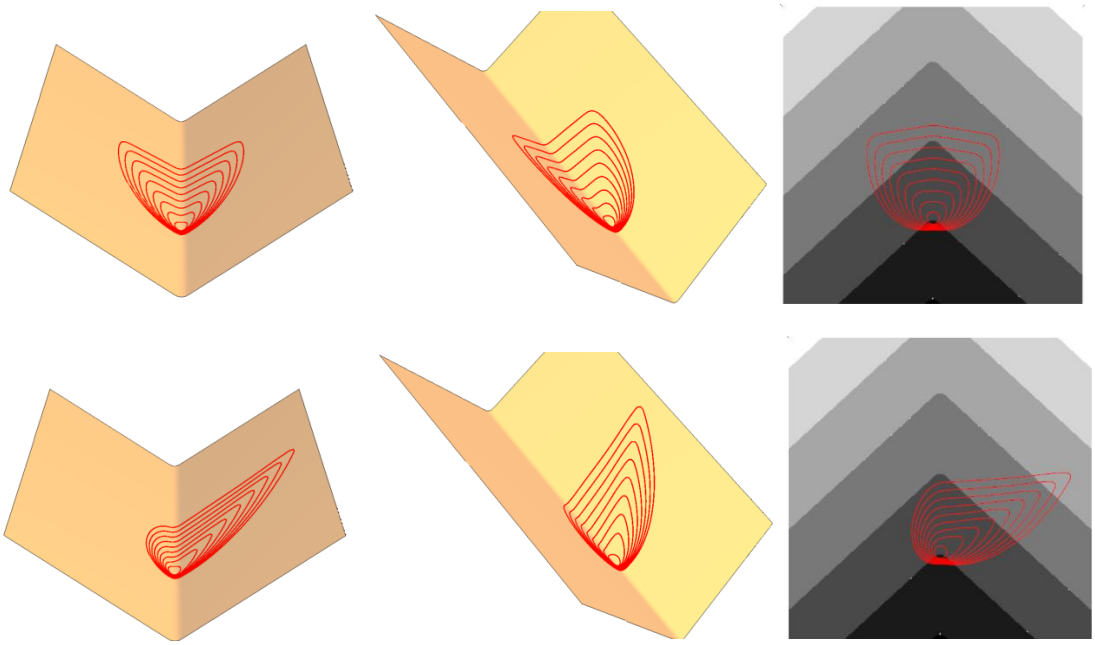

Figure 6 - Fire perimeter evolution in the valley. We consider homogenous fuel, geodesic and normal curvatures influence and the slope influence without the wind influence (top row) and considering the wind perpendicular to the valley (bottom row).

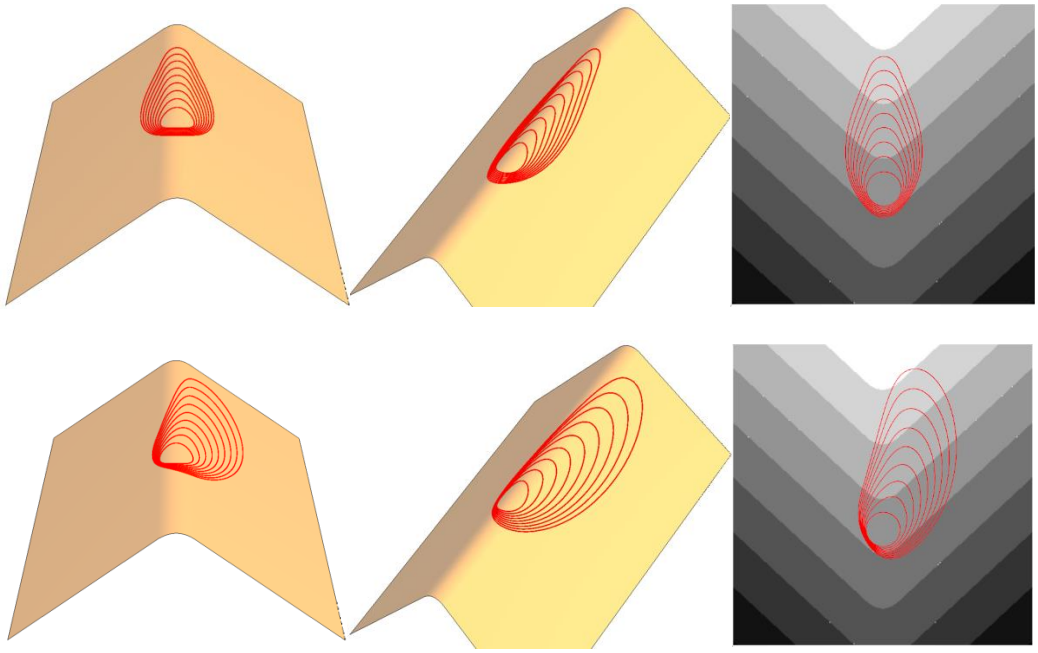

Figure 7 - Fire perimeter evolution on the ridge. We consider homogenous fuel, geodesic and normal curvatures influence and the slope influence without the wind influence (top row) and considering the wind perpendicular to the ridge (bottom row).

On the following examples, we present a simulations over a real topography of mountainous area of Staré Hory in central Slovakia. The fuel influence map was made from the forestry typological map

in resolution 0.83 m, consists of 4 colors and the rates of spread were assigned from (Prichard, et al., 2013) as follows

- black (roads, rivers) - non burnable,
- dark grey (broad-leaved forest) - 0.46 m.min^{-1},
- light grey (mixed forest) - 0.76 m.min^{-1},
- white (coniferous forest) - 1 m.min^{-1}.

The other model parameters can be estimated by an inverse modeling presented in (Ambroz, et al., Submitted). Following examples show the simulations considering various wind directions and various initial conditions.

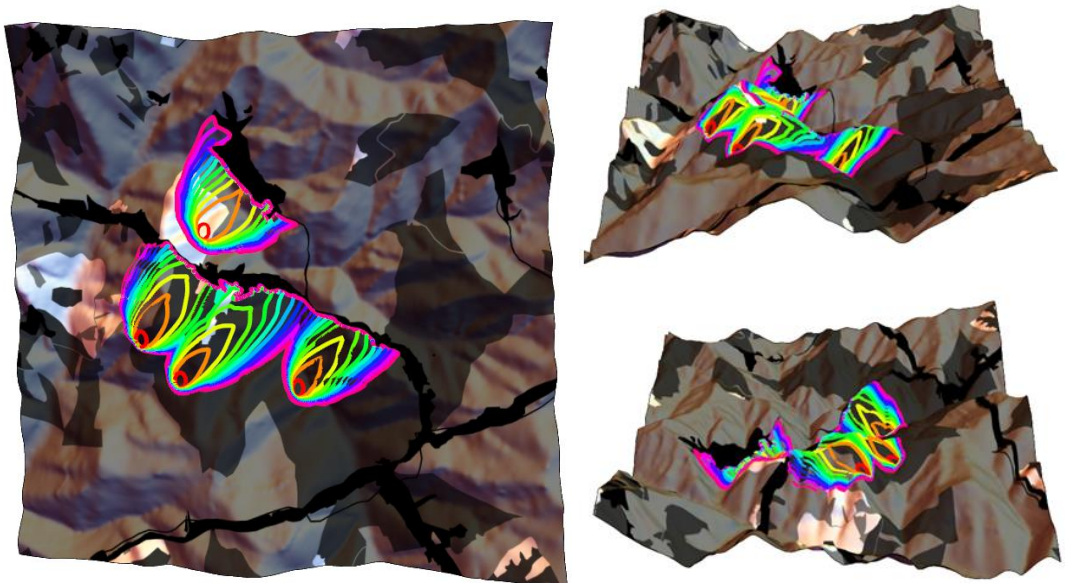

Figure 8 - ***Simulation with 4 initial fire perimeters (red) and their evolution in 1-hour intervals. On the left is the view from above, right top is view from south and right bottom is view from west. Wind is considered to be southwest at speed 4 m.min^{-1}. This simulation of 10 hour spread took 45 s of computational time.***

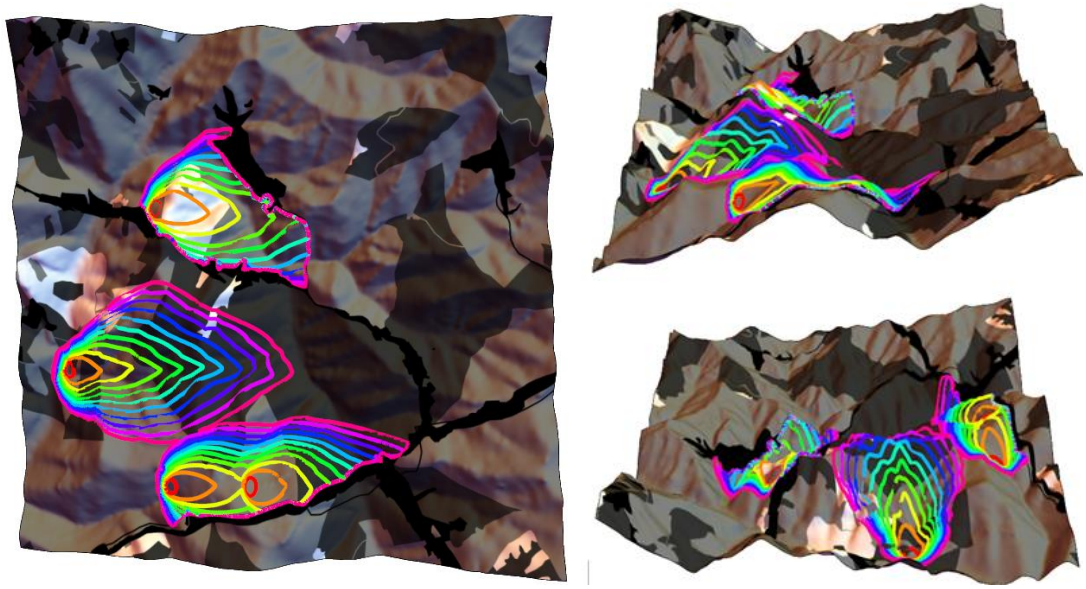

Figure 9 - ***Simulation with 4 initial fire perimeters (red) and their evolution in 1-hour intervals. On the left is the view from above, right top is view from south and right bottom is view from west. Wind is considered to be west at speed 4m.min^{-1}. This simulation of 10 hour spread took 49 s of computational time.***

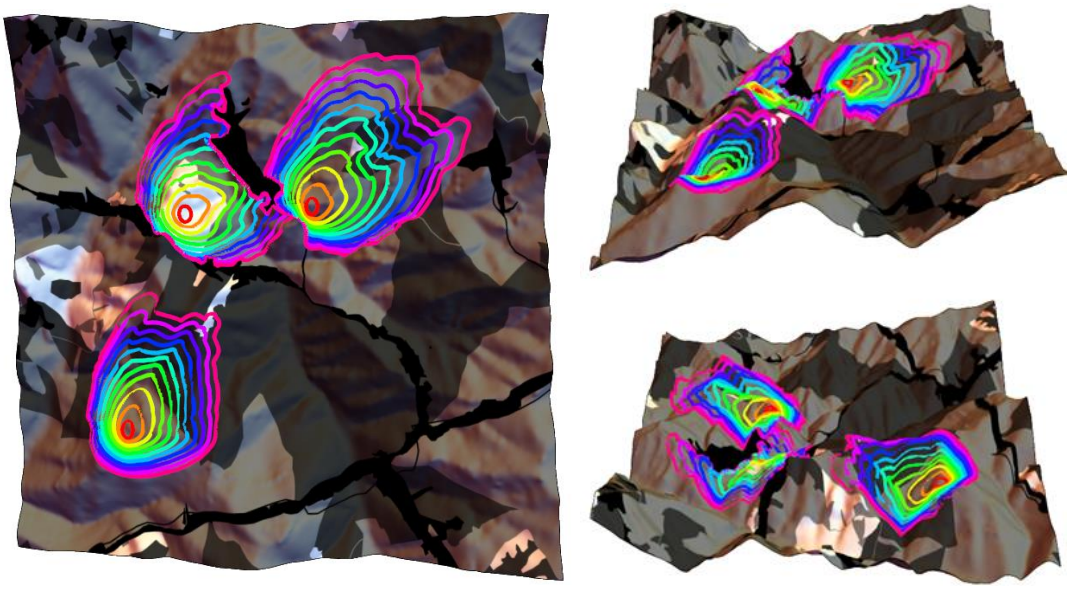

Figure 10 - Simulation with 4 initial fire perimeters (red) and their evolution in 1-hour intervals. On the left is the view from above, right top is view from south and right bottom is view from west. Wind is considered to be west at speed 1m.min^{-1}. This simulation of 10 hour spread took 53 s of computational time.

6. References

Ambroz, M., Balažovjech, M., Medľa, M. & Mikula, K., Submitted. Numerical modeling of wildland surface fire propagation by evolving surface curves. *Advances in Computational Mathematics.*

Balažovjech, M., Mikula, K., Petrášová, M. & Urbán, J., 2012. *Lagrangean method with topological changes for numerical modelling of forest fire propagation.* s.l., s.n., pp. 42-52.

Barrett, J., Garcke, H. & Nürnberg, R., 2009. Numerical approximation of gradient flows for closed curves in R^{d}. *IMA journal of numerical analysis,* 30(1), pp. 4-60.

Benninghoff, H. & Garcke, H., 2014. Efficient image segmentation and restoration using parametric curve evolution with junctions and topology changes. *SIAM Journal on Imaging Sciences,* Volume 7, pp. 1451-1483.

Butler, B. W., Anderson, W. R. & Catchpole, E. A., 2007. *Influence of slope on fire spread rate.* s.l., s.n., pp. 75-82.

Dziuk, G., 1999. Discrete anisotropic curve shortening flow. *SIAM Journal on Numerical Analysis,* Volume 36, pp. 1808-1830.

Hilton, J. E., Miller, C., Sharples, J. J. & Sullivan, A. L., 2017. Curvature effects in the dynamic propagation of wildfires. *Int. J. of Wildland Fire,* Volume 25, pp. 1238-1251.

Hou, T. Y., Lowengrub, J. S. & Shelley, M. J., 1994. Removing the stiffness from interfacial flows with surface tension. *J. of Comp. Physics,* Volume 114, pp. 312-338.

Krasnow, K., Schoennagel, T. & Veblen, T. T., 2009. Forest fuel mapping and evaluation of LANDFIRE fuel maps in Boulder County, Colorado, USA. *Forest Ecology and Management,* Volume 257, pp. 1603-1612.

Mikula, K., Ohlberger, M. & Urbán, J., 2014. Inflow-implicit/outflow-explicit finite volume methods for solving advection equations. *Applied Num. Math.,* Vol. 85, pp. 16-37.

Mikula, K. & Ševčovič, D., 2001. Evolution of plane curves driven by a nonlinear function of curvature and anisotropy. *SIAM J. on Applied Mathematics,* Volume 61, pp. 1473-1501.

Mikula, K. & Ševčovič, D., 2004. A direct method for solving an anisotropic mean curvature flow of plane curves with an external force. *Mathematical Methods in the Applied Sciences,* Volume 27, pp. 1545-1565.

Mikula, K. & Ševčovič, D., 2004. Computational and qualitative aspects of evolution of curves driven by curvature and external force. *Computing and Visualization in Science,* Volume 6, pp. 211-225.

Mikula, K. & Ševčovič, D., 2006. Evolution of curves on a surface driven by the geodesic curvature and external force. *Applicable Analysis,* Volume 85, pp. 345-362.

Mikula, K. & Urbán, J., 2012. *New fast and stable Lagrangean method for image segmentation.* s.l., s.n., pp. 688-696.

Osher, S. & Fedkiw, R., 2002. *Level Set Methods and Dynamic Implicit Surfaces.* s.l.:Springer New York.

Prichard, S. J. et al., 2013. *Fuel Characteristic Classification System Version 3.0: Technical Documentation,* s.l.: s.n.

Scott, J. H. & Burgan, R. E., 2005. Standard fire behavior fuel models: a comprehensive set for use with Rothermel's surface fire spread model. p. 66.

Sethian, J. A., 1999. *Level set methods and fast marching methods.* Cambridge university press.

Viegas, D., Pita, L. P., Matos, L. & Palheiro, P., 2002. *Slope and wind effects on fire spread.* Roterdam, Millpress.

Weber, R. O., 1989. Analytical models for fire spread due to radiation. *Combustion and flame,* Volume 78, pp. 398-408.